Branching in flow networks with linear congestion

Matthias Dahlmanns, Franz Kaiser, and Dirk Witthaut*
Forschungszentrum Jülich, Institute for Energy and Climate Research (IEK-STE), 52428 Jülich, Germany and Institute for Theoretical Physics, University of Cologne, Köln, 50937, Germany

(Received 20 December 2021; accepted 26 August 2022; published 23 December 2022)

In our modern world, we rely on the proper functioning of a variety of networks with complex dynamics. Many of them are prone to congestion due to high loads, which determines their operation and resilience to failures. In this article, we propose a fundamental model of congestion where travel times increase linearly with the load. We show that this model interpolates between shortest path and Ohmic flow dynamics, which both have a broad range of applications. We formulate the model as a *quadratic programme* and derive a generalization of Ohm's law, where the flow of every link is determined by a potential gradient in a nonlinear way. We provide analytic solutions for fundamental network topologies that elucidate the transition from localized flow to a branched flow. Furthermore, we discuss how to solve the model efficiently for large networks and investigate the resilience to structural damages.

DOI: 10.1103/PhysRevResearch.4.043208

I. INTRODUCTION

Modern societies rely on the proper functioning of various networks to provide elementary goods such as water, communication, electricity, or mobility. The operation and resilience of transportation networks thus plays an important role throughout different disciplines, ranging from biological systems [1–3] to manmade networks, such as hydraulic networks [4,5], power grids [6], and urban transportation systems [7,8].

Two models stand out in the analysis and simulation of transportation networks. The shortest path problem describes the flow of traffic in road or communication networks [9]. Each agent, car, or data package follows the shortest path from its origin to its destination. Several variants or extensions of this problem have been treated in the literature, including the famous traveling salesman problem [10], being highly influential in the development of graph algorithms and optimization methods (see, e.g, Refs. [11,12]). Ohm's and Kirchhoff's laws describe electric currents in resistor networks [13], real power flows in AC power grids [14] and water flow in hydraulic networks [4,5] or vascular networks [1–3]. The flow is generally distributed over all possible links, albeit at a different magnitude. The resilience of both types of networks has been intensively studied in the literature, see, e.g., Refs. [15,16] for shortest path networks and Refs. [17,18] for Ohmic networks.

In this article, we investigate a transportation network model that interpolates between shortest path and Ohmic flow. The model is inspired by traffic flow in the presence of congestion and generalizes the fundamental shortest path problem. As usual, the flow is determined to minimize the total travel time from a source to a target node. However, the travel time of every individual link increases with the flow due to congestion. The model is thus formulated as a convex *quadratic programme* (QP), that is a mathematically well studied class of optimization problems [19] which can be solved efficiently [20]. Furthermore, we provide a solution in terms of a nodal potential that generalizes Ohm's law: The flow over an edge is determined by the potential gradient, but the relation is no longer linear.

The model provides fundamental insights into the properties of network flows, showing when and where the network flow branches and how the network reacts to structural damages. Furthermore, congestion is a central limitation of real-world networks such as urban transport systems. These networks are becoming increasingly important due to the ongoing effort to reduce mobility-based carbon emissions to mitigate climate change. Also, an increasing share of the global population lives in cities which results in an rapidly growing usage of public transport systems. This raises the question how congestion impacts the performance and robustness of networks [21–24].

This article is organized as follows. First, in Sec. II, we formulate the linear congestion model and discuss possibilities to reduce the complexity of the problem. Then, in Secs. III and IV, we study the impact of congestion on two fundamental flow phenomena: first, the branching of the flow from one source to one sink and, second, the impact of a single link failure and the rerouting flow that is induced by this outage. We find that the flow locally behaves Ohmic up to a range that is growing with the strength of congestion. We present our conclusions in Sec. V and a more general benchmark in the Appendix.

II. A LINEAR MODEL OF CONGESTION

We propose a model that adopts congestion by adding a linear term to the flow cost function, which we denote by τ.

*d.witthaut@fz-juelich.de

The cost refers to the average travel time which the travelers inside the system try to minimize. Therefore, the expressions of cost and travel time are used synonymously throughout this manuscript.

We first establish the model and the basic notation before we discuss both the shortest path limit and the Ohmic limit. Then, the formalism is generalized to finite congestion using *Karush–Kuhn–Tucker* (KKT) conditions [19]. It turns out that this method is not suitable to find explicit solutions for the flows, but we can use a numerical solver by formulating our problem as a QP. It is, however, numerically expensive to solve a QP with high degrees of freedom. Therefore, we introduce a method to reduce the numerical complexity of the solution. We use the *numerically accurate sparsity-oriented QP solver* (NASOQ) [20] to solve our QP which makes use of the high sparsity in our system.

A. Formulation of the model

We consider a transportation network, consisting of a set of N nodes which are connected by a set of L edges on which travelers can move between nodes. We assume the network to be directed, that means for an edge l which starts at node n and ends at node m, denoted by (n, m) or l interchangeably, the flow F_l along the edge can only go from n to m. This implies in particular $F_l \geqslant 0$. If a flow between nodes n and m is possible in both directions, then this is encoded via two links (n, m) and (m, n).

We assume that the time τ_l which a traveler needs to travel along an edge l increases linearly with the local flow F_l, i.e.,

$$\tau_l(F_l) = (1 + \eta F_l) t_l, \tag{1}$$

where t_l is the travel time in case of vanishing flows, i.e., in absence of any congestion. We introduce the congestion parameter η which is the inverse of the flow intensity which doubles the travel time (i.e., which halfs the traveling velocity) along the link compared to the free-flow travel time t_l. Different edges might have different values of η. An example would be the case of distinguished lines in a metro network. In this case one would have edges that correspond to metro tunnels as well as edges that model the transfer from one line to another inside a station. These two types of edges might be differently prone to congestion. But these more complex scenarios are beyond the scope of this paper. Here, we assume that η is equal for all edges.

Traffic flow is fundamentally different from the flow of physical quantities such as water in a hydraulic network or current in an electric network. In the latter case, we only have to keep track of the net flow over a link or the net in- or outflow at a node in the network. In the case of traffic networks, we must take into account that travelers have individual starting points and destinations and cannot be set off against each other. Therefore, we restrict the analysis here to flows with a single starting point or a single destination, respectively. Travelers can enter or leave the network only at nodes, that correspond to stations in case of a public transportation network. We denote the inflow at node j by P_j, that is the number of travelers entering the network at this node. Traveler leaving the network are counted negatively.

Introducing the incidence matrix

$$I_{il} = \begin{cases} +1, & \text{if } l \text{ ends in } i, \\ -1, & \text{if } l \text{ starts in } i, \\ 0, & \text{else,} \end{cases} \tag{2}$$

which encodes the topology and orientation of the edges l in the network [25] allows us to write down the flow conservation law as

$$\sum_l I_{il} F_l = P_i, \tag{3}$$

where F_l is the flow on edge l. The continuity equation (3) is also referred to as Kirchhoff's current law (KCL) in circuit theory. The total travel time or cost τ reads

$$\tau = \sum_l \tau_l(F_l) F_l = \sum_l \left(F_l + \eta F_l^2\right) t_l.$$

We demand that the flows should arrange in such a way that they minimize τ under the boundary conditions imposed by Eq. (3). Considering furthermore the directedness constrains $F_l \geqslant 0$, the mathematical problem can be written as

$$\min_{F_l} \quad \sum_l \left(F_l + \eta F_l^2\right) t_l, \tag{4a}$$

$$\text{subject to} \quad \sum_l I_{il} F_l = P_i, \tag{4b}$$

$$F_l \geqslant 0. \tag{4c}$$

The objective function is a quadratic polynomial in L variables with N equality and L inequality constrains. Such a system is called a QP [19]. In general, solving a QP is NP-hard [26]. But if the objective function is convex, as it is the case in Eq. (4a), the problem can be solved in polynomial time [27].

B. Relation to other congestion models

Before we proceed to the results of our analysis, we briefly comment on the congestion model (1) and its correspondence to empiric data and other models. The choice of this equation follows two main motivations. First, it interpolates between the two most fundamental models of transportation and flow networks, the shortest-path and the Ohmic flow, and thus allows for essential insights into the relation of the two models. Second, the linear function in Eq. (1) can be viewed as the leading term in a Taylor approximation to a general function $\tau_l(F_l)$. Hence our results can be viewed as a generic first-order approximation to different types of congestion flows. We briefly review some examples of such flows below.

Road traffic is probably the most prominent example of congested flows. Macroscopic and economic models of road traffic often resort to the Bureau of Public Road functions [23],

$$\tau_l = t_l + f(F_l),$$

which are widely used in the literature [28,29]. The function f describes congestion. It is monotonically increasing with the flow F_l and satisfies $f(0) = 0$. Different function forms are used in the literature, with a fourth order power law being particularly popular.

In microscopic and empiric studies, congestion effects are typically analysed in terms of the vehicle density ρ. An early empiric study by Greenshields suggested that the average velocity v decreases approximately linearly as $v(\rho) \approx v_0 - a\rho$ [30]. Greenberg introduced fluid mechanics to model congested flows and obtained the expression $v(\rho) = c \times \log(\rho_{\text{jam}}/\rho)$ for large densities, with parameters obtained from fits to empiric data [31]. Helbing derived and validated a model for congestion in multilane traffic, where the average equilibrium velocity reads [32,33]

$$v(\rho) = v_0 - \rho \frac{\tau(\rho)[1 - p(\rho)\xi(\rho)]}{1 - \rho/\rho_{\max} - \rho T v(\rho)},$$

with ξ being the variance of car velocities, τ the relaxation time of acceleration, p the probability of overtaking, and T the reaction time of the drivers. Further developments have been reviewed in Refs. [34,35].

We can relate these results to our approach by interpreting the linear function (1) as a leading-order Taylor approximation. The travel time of a link of length L is given by $\tau = L/v(\rho)$ and the flow is written as $F = \rho v(\rho)$. We then express the derivative $d\tau/dF$ by $dv/d\rho$, both evaluated in the limit of vanishing traffic flow F, $\rho \to 0$. The travel time then reads

$$\begin{aligned}\tau(F) &= \tau(0) + \left[\frac{d\tau}{dF}\right]_{F=0} F + \mathcal{O}(F^2) \\ &= \tau(0) - \frac{L}{v_0^3 [dv/d\rho]_{\rho=0}} F + \mathcal{O}(F^2). \end{aligned} \tag{5}$$

Public transportation networks also suffer from congestion, which has received increasing attention in recent years [36]. As in the case of road traffic, congestion can lead to an increase in (expected) travel times, for instance through denied boarding or irregular vehicle arrivals [37]. Furthermore, the travel time is not the only factor that determines the decision for a certain route or mode of travel. The growing discomfort in overcrowded buses or trains substantially decreases the travelers' utility such that they may choose alternatives [37,38]. These effects have been confirmed by several empiric studies. However, the analysis is more involved as one has to quantify the travelers' behavior and not just the physical travel times [39–41]. In terms of our model, these effects can be taken to account by replacing the travel time (1) by a more general effective cost function, without altering the mathematical structure. Notably, the study [42] tries to quantify the negative effect of crowding in terms of an equivalent increase of travel times. In the data analysis the authors use a linear model just as Eq. (1) in comparison to other functional forms.

Finally, effects of congestion are also investigated in biological flow networks. For instance, oxygen transport in vertebrates show congestion in terms of hematocrit: The transport flux first increases with the volume concentration before it saturates and decreases again [43]. Similar relations of flux and concentration are also found in different modes of drinking [44]. An excellent review of different types of transportation systems, including a comparison of biological and traffic flows, is provided in Ref. [45].

C. Shortest path limit and Ohmic limit

In the limit $\eta = 0$, the quadratic terms in the objective function vanish and we obtain a *linear programme* (LP) where it remains to minimize $\tau(F_l) = \sum_l t_l F_l$. This setup is known as the *shortest path problem* [9], we will therefore refer to this limit as the shortest path limit. Shortest path problems can be solved using Dijkstra's algorithm [46].

In the limit $\eta \to \infty$, the linear terms in the objective function vanish so that it remains to minimize $\tau(F_l) = \sum_l t_l F_l^2$. The objective function $\tau(F_l)$ is in this limit identical to the objective in Ohmic networks such as electrical power grids [13, chap. IX, Theorem 1]. Using the notion of undirected networks, the problem becomes particularly simple to solve: In networks, where for each edge (n, m) the counter edge (m, n) also exists with identical $t_{nm} = t_{mn}$, we can consider each of these edge pairs as a single where flow can go in both directions so that we can omit the inequality constrains (4c) and obtain the following optimization problem:

$$\min_{F_l} \sum_l t_l F_l^2, \tag{6a}$$

$$\text{subject to } \sum_l I_{il} F_l - P_i = 0. \tag{6b}$$

This problem can be solved using the method of Lagrange multipliers [47]: In this formalism, we introduce for each constrain a Lagrange multiplier λ_i and define the Lagrangian

$$\mathcal{L} = \tau - \sum_i \lambda_i \left(\sum_l I_{il} F_l - P_i \right).$$

For the optimal set of flows F_l, the Lagrangian $\mathcal{L}$ must be stationary, i.e.,

$$\partial_{F_l} \mathcal{L} = \partial_{F_l} \tau - \sum_i \lambda_i I_{il} = 2 t_l F_l - \sum_i \lambda_i I_{il} \stackrel{!}{=} 0.$$

We therefore get

$$F_l = \frac{\sum_i \lambda_i I_{il}}{2 t_l} = \kappa_l \sum_i \lambda_i I_{il}, \tag{7}$$

with $\kappa_l := (2t_l)^{-1}$. Let us rewrite this relation in a slightly different form. For a link $l = (n, m)$ that connects two nodes n and m, the flow reads

$$F_{n \to m} = \frac{\lambda_n - \lambda_m}{2 t_{nm}}. \tag{8}$$

We thus recover Ohm's law if we identify λ_n as the voltage at node n and $2t_{nm}$ as the resistance of the link (n, m). Thus, we will henceforth refer to the limit $\eta \to \infty$ as the Ohmic limit.

To determine the λ_i, we insert Eq. (7) into the boundary conditions (6b). Using the properties of I_{il} we find

$$\sum_j \kappa_{ij} (\lambda_i - \lambda_j) = P_i. \tag{9}$$

Introducing the Laplacian matrix $L \in \mathrm{R}^{n \times n}$ with elements

$$L_{ij} = -\kappa_{ij} + \left(\sum_k \kappa_{ik} \right) \delta_{ij},$$

this problem can be written as

$$\sum_j L_{ij}\lambda_j = P_i, \tag{10}$$

which can be solved by multiplying from the left with the (pseudo)inverse matrix $(L^{-1})_{ij}$:

$$\lambda_i = \sum_j (L^{-1})_{ij} P_j. \tag{11}$$

Finally, we obtain the flows F_l in the Ohmic limit by inserting Eq. (11) into Eq. (7).

D. Generalization to finite congestion

The previous approach of solving the optimization problem in the limit $\eta \to \infty$ via Lagrange multipliers can be generalized to the case of finite $\eta > 0$ and directed networks using the theorem of Karush-Kuhn-Tucker (KKT) [19, chap. 5.5.3] which generalizes the formalism of Lagrange multipliers: Considering the optimization problem (4) for a network with N nodes and L edges, we introduce the generalized Lagrangian

$$\mathcal{L}(F_l, \lambda_i, \mu_l) := \underbrace{\sum_l \left(F_l + \eta F_l^2\right) t_l}_{\equiv \tau(F_l)} - \sum_i \lambda_i \left(\sum_l I_{il} F_l - P_i\right) - \sum_l \mu_l F_l.$$

The KKT conditions then read

$$\partial_{F_l} \mathcal{L} = (1 + 2\eta F_l) t_l - \sum_i \lambda_i I_{il} - \mu_l = 0, \tag{12a}$$

$$\sum_l I_{il} F_l - P_i = 0, \tag{12b}$$

$$F_l \geqslant 0 \ \ \forall\, l, \tag{12c}$$

$$\mu_l \geqslant 0 \ \ \forall\, l, \tag{12d}$$

$$\mu_l F_l = 0 \ \ \forall\, l, \tag{12e}$$

with $i = 1, \ldots, N$ and $l = 1, \ldots, L$. For the optimal flows F_l, the gradient of the Lagrangian $\mathcal{L}$ must vanish. Thus, solving Eq. (12a) for F_l and considering the constraints (12c), we find

$$F_l = \begin{cases} \frac{1}{2\eta t_l} \sum_i (\lambda_i I_{il} + \mu_l - t_l), & \text{if positive,} \\ 0, & \text{else.} \end{cases}$$

Using Eq. (12e), we can omit μ_l as it has to be zero if $F_l \neq 0$. Hence, using the Heaviside function $\Theta(x)$ we can write

$$F_l = \frac{\sum_i \lambda_i I_{il} - t_l}{2\eta t_l} \Theta\left(\frac{\sum_i \lambda_i I_{il} - t_l}{2\eta t_l}\right).$$

Considering $l \mathrel{\hat{=}} (n, m)$, i.e., let edge l start at node n and end at node m, using the definition of I_{il} in Eq. (2) and introducing the matrix of capacities

$$\kappa_{nm} := \begin{cases} \frac{1}{2\eta t_{n\to m}}, & \text{if link } (n, m) \text{ exists,} \\ 0, & \text{otherwise,} \end{cases} \tag{13}$$

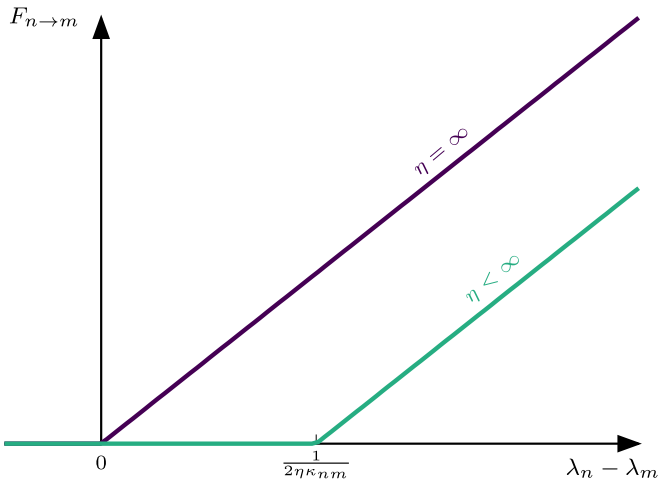

FIG. 1. The flow $F_{n\to m}$ along an edge from node n to node m in dependence of the potential drop $\lambda_n - \lambda_m$ in the Ohmic limit $\eta = \infty$ and for finite congestion $\eta < \infty$. For positive potential drop and $\eta = \infty$, the flow is directly proportional to $\lambda_n - \lambda_m$, for negative potential drops it is zero. For finite congestion η, the curve is shifted to the right.

this becomes

$$F_{n\to m} = \left[\kappa_{nm}(\lambda_n - \lambda_m) - \frac{1}{2\eta}\right] \Theta\left[\kappa_{nm}(\lambda_n - \lambda_m) - \frac{1}{2\eta}\right]. \tag{14}$$

Inserting Eq. (14) into Eq. (12b) yields

$$\begin{aligned} P_i &= \sum_l I_{il} F_l = \sum_{j:\exists(i,j)} F_{i\to j} - \sum_{j:\exists(j,i)} F_{j\to i} \\ &= \sum_j \left[\kappa_{ij}(\lambda_i - \lambda_j) - \frac{1}{2\eta}\right] \Theta\left[\kappa_{ij}(\lambda_i - \lambda_j) - \frac{1}{2\eta}\right] \\ &\quad - \sum_j \left[\kappa_{ji}(\lambda_j - \lambda_i) - \frac{1}{2\eta}\right] \Theta\left[\kappa_{ji}(\lambda_j - \lambda_i) - \frac{1}{2\eta}\right]. \end{aligned} \tag{15}$$

Note that we recover Eq. (9) for undirected networks, i.e., $\kappa_{ij} = \kappa_{ji}$, in the Ohmic limit $\eta \to \infty$ with $\kappa_{ij}^{-1} \propto \eta t_{i\to j}$ kept finite.

Thus, also for finite congestion $\eta < \infty$, we can interpret the λ_i as potentials like in the Ohmic limit. In Fig. 1, the flow $F_{n\to m}$ along an edge from n to m is plotted over the potential drop $\lambda_n - \lambda_m$ over this edge. In the limit $\eta \to \infty$, we find a straight line, i.e., the flow is proportional to the potential drop in the Ohmic limit. For finite congestion, $\eta < \infty$, we observe a plateau for $\lambda_n - \lambda_m < t_{n\to m}$ due to the Heaviside function in Eq. (14). Thus, a finite free-flow travel time $t_{n\to m}$ suppresses the flow on the edge up to a critical value of the potential drop $\lambda_n - \lambda_m$. In the limit $t_{n\to m} \to 0$ the $1/2\eta$ term inside the Heaviside function becomes negligible such that the argument is always positive if the potential drop $\lambda_n - \lambda_m$ is.

The formalism of Lagrange multipliers is very helpful to get insights to study fundamental properties of the system. However, the resulting equations (15) are nonlinear and even nonanalytic in the potentials λ_i, which regularly causes problems for numerical solvers. Therefore, we use an algorithm

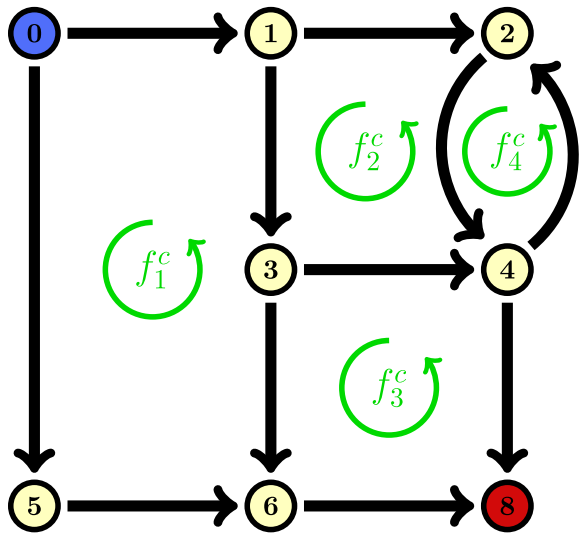

FIG. 2. Sketch of a network with loops. Each loop adds a new degree of freedom on how the flows can arrange that can be visualized as cycle flows f_1^c which flow around each loop. Note that when having two edges connecting the same nodes we get also for each of these 2-loops a d.o.f. like f_4^c.

that directly solves the quadratic programme numerically to obtain the optimal flows.

E. Reducing the numerical complexity using an adapted Hardy Cross method

The optimization problem (4) can be solved directly using a numerical QP solver. However, the solution becomes numerically expensive for large systems as the runtime is polynomial in the number of edges L of the system. To reduce the numerical complexity, we can make use of Kirchhoff's current law which reduces the degrees of freedom of the system.

If the network is a tree, then the flows are fully determined by flow conservation (4b). For each closed loop in the network, a new degree of freedom arises for the arrangement of flows so that they are not violating Kirchhoff's current law. As sketched in Fig. 2, we can consider these degrees of freedom as cycle flows which are added to the initial flow on each edge with parallel orientation on the loop and subtracted from the flows on edges along the loop where the orientation is antiparallel.

With these thoughts, we can partially solve the problem using a method inspired by the Hardy Cross method [48], which was originally developed to calculate flows in pipe networks. The method involves the following steps:

(1) find an arbitrary set of flows $F_{l,0}$ which fulfils Kirchhoff's current law (4b) at each node.

(2) add for each fundamental loop a cycle flow f_i^c flowing along the edges which form the loop. If the orientation of f_i^c and edge l are parallel, then f_i^c is added to the $F_{l,0}$. When they are antiparallel, it is subtracted.

(3) find the set of f_i^c which minimizes τ and fulfils the inequality boundary conditions $F_l \geqslant 0$.

To formalise this method, we introduce the cycle incidence matrix C_{li} with the components

$$C_{li} = \begin{cases} +1, & \text{if edge } l \text{ is parallel to loop } i, \\ -1, & \text{if edge } l \text{ is antiparallel to loop } i, \\ 0, & \text{if edge } l \text{ is not in loop } i. \end{cases} \tag{16}$$

Using this definition, the resulting flows $F_l(f_i^c)$ after adding the cycle flows f_i^c to the initial guess $F_{l,0}$ read

$$F_l\left(f_i^c\right) = F_{l,0} + \sum_i C_{li} f_i^c. \tag{17}$$

The system can now be written as

$$\min_{f_i^c} \tau\left[F_l\left(f_i^c\right)\right],$$

$$\text{subject to } F_l\left(f_i^c\right) = F_{l,0} + \sum_i C_{li} f_i^c \geqslant 0.$$

When we insert Eq. (17) into Eq. (4a), we find

$$\tau\left[F_l\left(f_i^c\right)\right] = \frac{1}{2}\sum_{i,j} f_i^c \beta_{ij} f_j^c + \sum_i \alpha_i f_i^c + \tau(F_{l,0}), \tag{18}$$

with the symmetric matrix

$$\beta_{ij} = 2\eta \sum_l t_l C_{li} C_{lj}, \tag{19}$$

the vector

$$\alpha_i = \sum_l t_l (1 + 2\eta F_{l,0}) C_{li}, \tag{20}$$

and the constant expression $\tau(F_{l,0})$ that does not depend on the cycle flows f_i^c and can therefore be omitted in the following discussion.

We find the objective function to be again a quadratic polynomial so that the remaining system is also a QP:

$$\min_{f_i^c} \frac{1}{2}\sum_{i,j} f_i^c \beta_{ij} f_j^c + \sum_i \alpha_i f_i^c, \tag{21a}$$

$$\text{subject to } F_l\left(f_i^c\right) = F_{l,0} + \sum_i C_{li} f_i^c \geqslant 0. \tag{21b}$$

While the initial QP was of order L with N equality and L inequality constrains, the new QP is only of order n_l with zero equality and L inequality constrains where n_l is the number of loops in the network. Furthermore, the matrix β_{ij} is hermitian and positive-definite. Hence, the system (21) is again a convex QP that can be solved in polynomial time.

Considering real-world networks like the Cologne tram network [49], there are much fewer loops than number of links, i.e., $n_l \ll L$, if we consider each connection between two stations as a link. Without considering different lines, in the Cologne tram network we find 219 connections and only 18 loops. In addition to these large loops we must also consider that each connection in this network consists of two edges—one for each direction. Thus, we get additional 219 loops consisting out of the antiparallel edges connecting the same two nodes. In the end, this means that the original QP is of order $L = 438$ while the reduced QP with the adapted Hardy Cross method is only of order $n_l = 237$, i.e., we can almost half the degrees of freedom.

F. Further reduction of complexity

In the example of the previous section, 219 of 237 degrees of freedom in Eq. (21) are caused by the antiparallel edges in the network. Thus, the large majority of the remaining degrees of freedom when using the adapted Hardy Cross method originate in the fact that along all links in the network one can go in both directions. However, when minimizing the average travel time τ we know that the flow along one of these two edges must be exactly zero as we could reduce τ otherwise by adding an appropriate cycle flow along these two edges to cancel out one of these flows.

Since we observe a large number of such bidirectional connections between nodes in most transport networks, an appropriate handling of these flows can further reduce the number of free parameters that need to be solved for. In the example of the Cologne tram network, only 18 degrees of freedom would remain.

The crucial point when solving a convex QP is to find the active set of inequalities (21b). In our system, that corresponds to the flows F_l that are exactly zero. We know that in the case of two antiparallel edges, at least on one of them, the flow must vanish. Using this knowledge would therefore tremendously reduce the complexity of finding the correct active set.

III. BRANCHING OF NETWORK FLOWS

For shortest path limit $\eta = 0$, the flow between two nodes in the network flows along a single path if it is unique. In the Ohmic limit $\eta \to \infty$, however, the flow always spreads over all paths from the source to the sink. This raises the question, how does the transition take place when driving the congestion parameter η? When and how does the flow branch?

In this section, we discuss the branching of the flow on a regular lattice and on a irregular, real network topology. For the fundamental 2×3 square lattice, we derive analytic expressions for the optimal flows in dependence of the congestion parameter η, while we rely on a QP solver to solve Eq. (4) numerically for general network topologies.

A. A fundamental example of branching

We first discuss a fundamental network topology to study the impact of congestion on the optimal flow pattern. We choose a system that is symmetric and has only two effective degrees of freedom and thus allows for an analytic solution. Consider a 2×3 square lattice with identical edges and a source-sink pair of strength P in the center of the lattice as sketched in Fig. 3(a). Numbering the nodes consecutively from top left to bottom right, Kirchhoff's current law (4b) reads

$$F_{3\to1} = F_{1\to2} = F_{2\to4},$$
$$F_{3\to5} = F_{5\to6} = F_{6\to4},$$
$$F_{3\to1} + F_{3\to4} + F_{3\to5} = P.$$

Due to the mirror symmetry of the system, the flow along the upper and lower branch must be equal. Thus, we have only two effective degrees of freedom,

$$F_2 := F_{3\to1} = F_{1\to2} = F_{2\to4} = F_{3\to5} = F_{5\to6} = F_{6\to4},$$
$$F_1 := F_{3\to4},$$

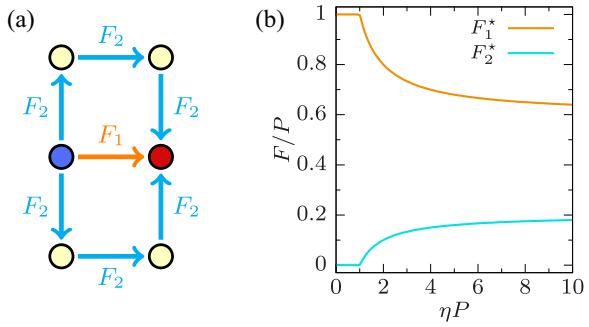

FIG. 3. Optimal flow on a 2×3 square lattice in presence of congestion. (a) We consider the case of a source (blue) and a sink (red) with an inflow and outflow of P, respectively. We can split the flow due to symmetry into two components F_1, which takes the direct link, and F_2, which takes the upper and lower branch. (b) The optimization problem (21) can be solved directly and we find analytic expressions for both flow components as a function of the congestion parameter η. Below a critical value of $\eta_c = 1/P$, the flow on the longer branches (F_2) is exactly zero.

that must satisfy the condition

$$F_1 + 2F_2 = P. \tag{22}$$

Furthermore, both F_1 and F_2 must be nonnegative as there would be a flow from the sink back to the source otherwise. This yields $F_1, F_2 \in [0, P]$. Using these restrictions, we can directly solve Eq. (4a) by imposing Eq. (22) and find the optimal flow

$$F_2^\star(\eta) = \begin{cases} 0, & \eta < 1/P, \\ \frac{P-1/\eta}{5}, & \eta \geqslant 1/P, \end{cases} \tag{23}$$

that minimizes the total travel time. The optimal flow $F_1^\star$ on the direct link is obtained by plugging Eq. (23) into Eq. (22). Note, that this result can be written independently of the source strength P when rescaling $\eta \to \eta P$ and writing the flow in units of P, $F_i \to F_i/P$. In Fig. 3(b), the optimal flows $F_1^\star$ and $F_2^\star$ are plotted over the strength of congestion η.

We find that the long branches only carry flow for $\eta > 1/P$ so that we can define the critical value of the congestion parameter $\eta_c = 1/P$, below which we observe a flow only on the shortest path while above this value, the flow splits up on more branches. That is, branching becomes favourable only if $\eta > \eta_c$. We thus find a pure shortest path flow also for weakly congested flows.

In the Ohmic limit $\eta \to \infty$, the flows smoothly converge to $F_2^\star = 0.2P$ and $F_1^\star = 0.6P$.

In the Appendix, we conduct in more details the calculations for the optimal flow in a 2-node network with two concurrent branches with different ratios of the branch weights. We find that the critical value of the congestion parameter η_c in general grows linearly with the weight ratio t as

$$\eta_c(t) = \frac{t-1}{2}\frac{1}{P}. \tag{24}$$

Note, that the result from Eq. (23) is recovered when inserting the ratio of the path weights on the square grid, that is $t = 3$.

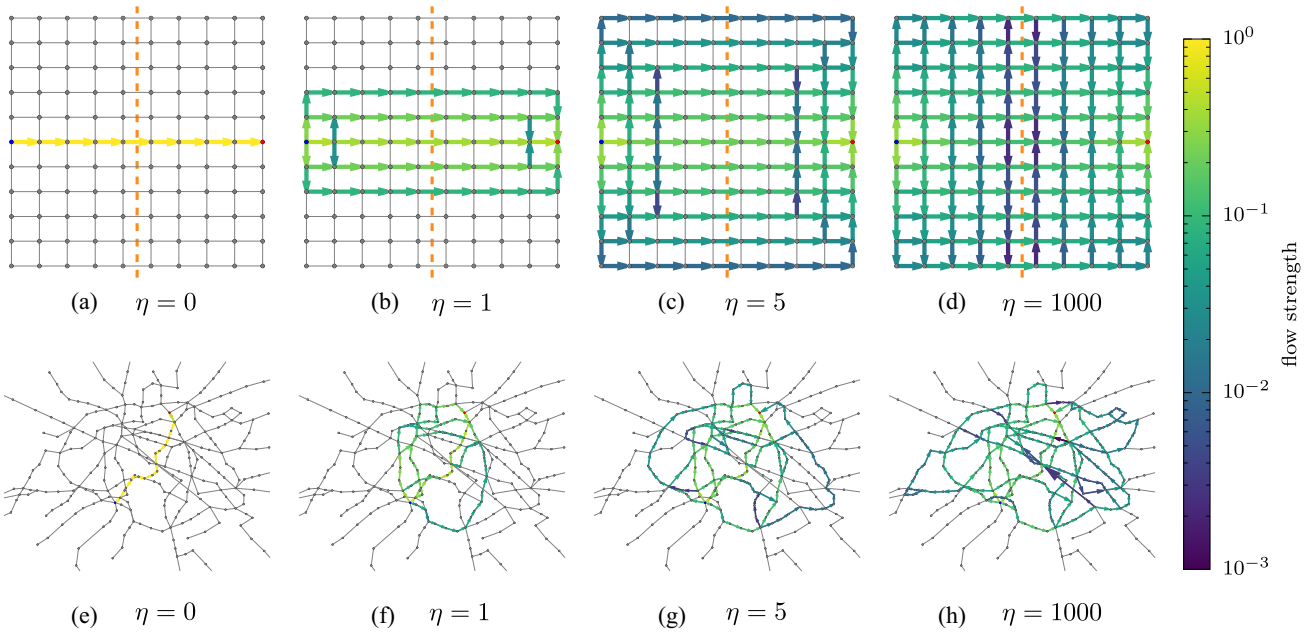

FIG. 4. Branching in dependence of congestion. For both a regular square lattice (a)–(d) and the irregular topology of the Paris metro network (e)–(h), we find an increasingly complex flow pattern with growing strength of congestion η. In the shortest path limit $\eta = 0$, all the flow only takes the shortest path (a), (e) while in the Ohmic limit for very strong η, all available paths are affected by the flow (d), (h).

B. Branching on large networks

In the previous section, we found that the flow is branching for η larger than a critical η_c that depends on the network geometry. We now study the impact of congestion on the flow pattern on larger networks for which it is not feasible anymore to solve Eq. (4) by hand. In particular, we consider the branching of flow between a single source-sink pair of unit strength $P = 1$ both on a square grid and in a real network topology, namely the Paris metro network. The effective "crowding costs" in the Paris metro system have been analysed in socioeconomic experiments, in particular for the heavily loaded lines 1 and 4 [50]. These experiments aim to quantify the impact of congestion on the travelers' preferences for a certain route or mode of transport—for instance via an equivalent increase of travel times [42].

On the square grid, we assume the source and sink to the located vertically centered and horizontally at the opposite ends of the grid. In Figs. 4(a)–4(d), the optimal flow pattern on a 10×11 grid is visualized for different strengths of congestion η.

We finds that in the limit of no congestion, $\eta = 0$ [Fig. 4(a)], all the flow is only taking the shortest path from the source to the sink, as expected. When increasing the strength of congestion η, we observe that the flow expands to more and more alternative paths until it fills all links in the $\eta \to \infty$ limit [Fig. 4(d)].

The flow patterns for the same values of η is shown in Figs. 4(e)–4(h) in the Paris metro network where all travelers enter the metro at Gare Montparnasse and leave the network at Gare du Nord. Again, with increasing η, the flow spreads over more and more alternative routes: In the shortest path limit $\eta = 0$, all travelers take the direct connection (which corresponds to the metro line 4). In the presence of congestion, alternative routes such as the lines 5 or 13 for $\eta = 1$ and in addition the ring lines 2 and 6 for $\eta = 5$ become involved. In the extreme case $\eta = 1000$, almost all paths connecting the starting point and the destination are used by the flow. Note that in this simple model we neglected the time loss when changing from one metro line to another.

The simulation results suggest that, in periods of strong congestion, some travelers avoid the overcrowded lines through the city center and rather take a detour via the periphery. Hence, spatial traffic patterns should change during the day, with traffic in the periphery increasing more than proportional during rush hour. However, it remains highly challenging to confirm this hypothesis in practice for two reasons: First, high-resolution data on public transport utilization is generally sparse. Second, route choices are affected by a variety of features impeding any causal interpretation. In the case of car traffic, some statistical results on spatiotemporal traffic patterns are available (see Ref. [51] and references therein).

To further quantify the branching, we return to the square grid and study the flow profile along the axis perpendicular to the main flow direction, along the dashed vertical line in Figs. 4(a)–4(d). In Fig. 5(a), The flows are plotted over the distance d to the shortest path in the center of the lattice for different values of η on a 10×51 square lattice.

We find that the flows close to the shortest path converge very fast with increasing η and roughly scales with $F(d) \propto 1.4^{-|d|}$. For each value of η, we find a sharp cutoff range r beyond which the flow is exactly zero. In Fig. 5(b), the cutoff range for the 10×51 lattice is plotted over the congestion parameter η. We find an approximate scaling of $r(\eta) \propto \eta^{1/4}$.

IV. SUSCEPTANCE TO LINK FAILURE

In network science, the stability and resilience against damages is an important issue and intensively studied for

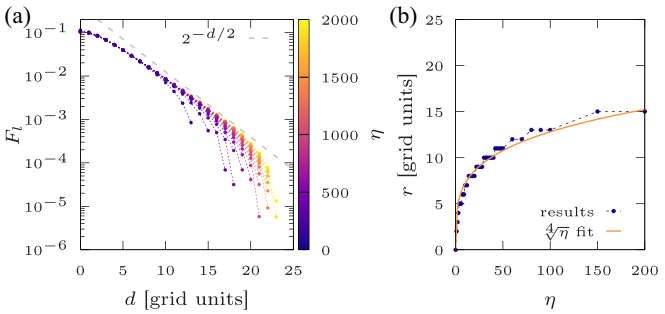

FIG. 5. Branching profile on a 10×51 lattice. (a) The flow F perpendicular to the main flow direction in the center of the lattice, as marked in Figs. 4(a)–4(d), over the distance d from the shortest path for different strengths of congestion η. For a distance d larger than the cutoff range r, all flows are exactly zero. In (b) the cutoff range is plotted over η.

various types of networks [6,17,18,52]. There are different types of damages that can occur. They might cause a reductions in capacity up to the complete failure of one or multiple links. In this paper, we focus on the complete failure of a single link that is realised by removing the failing link from the network. In transport networks, these outages frequently occur due to accidents, tempests or technical defects. When planning a transport network, it is therefore important to study the rerouting pattern, that is the difference in the flow caused by the removal of a link, to spot critical links that might dramatically impact certain network areas in case of an outage.

We discuss the rerouting flows again on a square lattice, where a source-sink pair is located next to each other in the center of the grid as shown in Fig. 6. The rerouting flow ΔF_l on an edge l is the difference between the flow in the full lattice F_l^{full} and the flow after the outage F_l^{out}:

$$\Delta F_l := F_l^{\text{out}} - F_l^{\text{full}}. \tag{25}$$

Hence, ΔF_l is a measure how strong edge l is affected by this outage. In Fig. 6, the flow pattern are visualized for $\eta = 10$ and for both the full lattice [Fig. 6(a)] and the lattice after the outage of the central link [Fig. 6(b)]. In Fig. 6(c), the corresponding rerouting flow ΔF_l is shown.

We notice that as a consequence of the outage of the central link, the range of edges, which are affected by the flow, can grow. In the case of $\eta = 10$, we find that after the outage, one additional shell around the center is affected by the flow. Hence, we can conclude that the failure of the link may extend the range of flow. Considering a network with multiple flows between different source-sink pairs, this can evoke interference between different flow layers in case of a link failure even if the flows do not cross each other when the network is fully functional.

To quantify the impact of the strength of congestion η on the rerouting flow, we again consider the parallel flow profile over the distance d to the failing link as highlighted by the dashed line in Fig. 6(c).

We find the rerouting flow ΔF_l in distance d to the failing link to decrease with d^{-2} as shown in Fig. 7(a), until it approaches a cutoff distance r beyond which the ΔF_l are exactly zero. A similar investigation for electrical power grids,

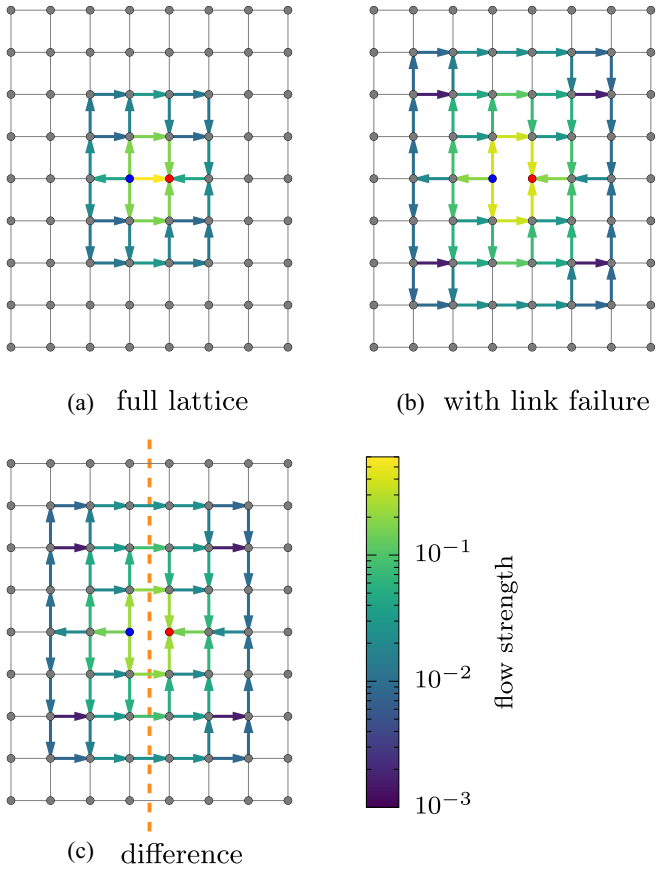

FIG. 6. Rerouting flow in case of a link failure. The impact of a single link failure on the network is studied on a square lattice with the source-sink pair laying on neighboring nodes in the center of the lattice. This scenario is illustrated for $\eta = 10$: (a) the optimal flow in the full lattice, (b) the optimal flow with the link failure, i.e., after removing the central link that directly connects source and sink. (c) the rerouting flow, i.e., the difference between the flow after the link failure and the flow in the full lattice. To discuss the rerouting flow pattern, we consider the flow differences on the edges in parallel to the failing link, marked by the dashed line in c

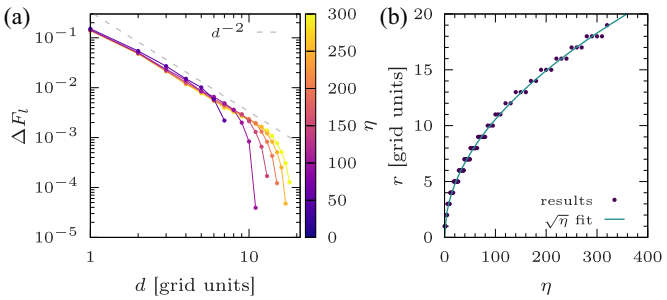

FIG. 7. Profile of the rerouting flow in presence of congestion. (a) The strength of the rerouting flow ΔF_l decreases as a power law d^{-2} with the distance d from the failing link up to a sharp cutoff distance r, beyond which the rerouting flow is exactly zero. (b) The cutoff range r, i.e., the distance of the last link that still carry any flow from the failing link, grows with $\sqrt{\eta}$.

that correspond to the $\eta \to \infty$ in our case, revealed also a $\Delta F_l \propto d^{-2}$ scaling [17]. We can therefore conclude that in this linear congestion model, the optimal flow locally looks similar to the Ohmic flow for distances $d < r$ while it is exactly zero for $d > r$.

In Fig. 7(b), we plotted this flow range r for various η and found a very accurate $r \propto \sqrt{\eta}$ scaling. This scaling law can be explained using the Lagrange multiplier λ_n, that define a potential for each node n. In Eq. (14), we found the flow $F_{n\to m}$ from n to m can be written as

$$F_{n\to m} = \left[\kappa_{nm}\Delta\lambda_{nm} - \frac{1}{2\eta}\right]\Theta\left(\kappa_{nm}\Delta\lambda_{nm} - \frac{1}{2\eta}\right)$$

in terms of the potential drop $\Delta\lambda_{nm} := \lambda_n - \lambda_m$. Below the critical potential drop $\Delta\lambda^C_{nm} = \kappa_{nm}/2\eta \propto \eta^{-1}$, the flow is exactly zero.

Although we cannot determine the potentials λ_n directly, we know the potential drop scales with $\Delta\lambda_{nm} \propto F_{n\to m} \propto d^{-2}$ for $\Delta\lambda_{nm} > \Delta\lambda^C_{nm}$. The cutoff distance r is reached when $\Delta\lambda_{nm}(r) = \Delta\lambda^C_{nm} \propto \eta^{-1}$. We therefore get $r^{-2} \propto \eta^{-1}$ which is equivalent to $r \propto \sqrt{\eta}$. Thus, the cutoff distance r must grow with the square root of the congestion parameter $\sqrt{\eta}$.

V. CONCLUSION

Transportation networks are increasingly prone to congestion. In this paper, we proposed a fundamental model that implements congestion as a linear increase in the time needed to travel along an edge caused by the local flow.

Mathematically seen, this model interpolates between ordinary shortest-path flows in case of no congestion and Ohmic flows, as in electrical power grids, in the limit of strong congestion. We note, however, that the analogy to the flows in electrical power grids only holds as long as we restrict to a single start or destination. In real transport networks, we frequently observe a large number of intersecting flows. In electrical power grids, these flows can be counted up and Kirchhoff's law only must hold for the overall flow. However, in a transportation network, we must ensure that Kirchhoff's current law is fulfilled for every single flow to ensure all travelers reach their individual destination.

We found that the minimal strength of congestion at which branching becomes favourable grows linearly with the weight ratio of the second shortest and the shortest path. As the strength of congestion is increasing, the flow is branching over more and more available paths until it affects the entire network in the limit of strong congestion. On the square grid, we found that the range of affected paths is growing with the fourth square-root of the congestion parameter leading to a strong increase of the range in the weak congestion regime. In the future, it would be interesting to study the topology of optimal network designs or optimal network extensions to relive the impact of congestion.

In our everyday life, networks are often prone to unforeseeable damages that might lead to the complete failure of a link in the network. To ensure the resilience of a network against damages, the impact of such an outage needs to be investigated. In this paper, we therefore studied the rerouting flow caused by the outage of a single line on a regular lattice. We found that the rerouting flow for finite congestion is locally similar to the rerouting flow in Ohmic networks and decays with a inverse-square law over the distance to the failing link. At a distance growing with the square root of the congestion strength, we observe a sharp cutoff beyond which the flow is exactly zero, which can be explained using Lagrange multipliers, although we could not determine these multipliers explicitly. Using this local similarity, we can profit from the extensive amount of research done for Ohmic flow networks, such as electrical power grids, to study strongly congested flow networks.

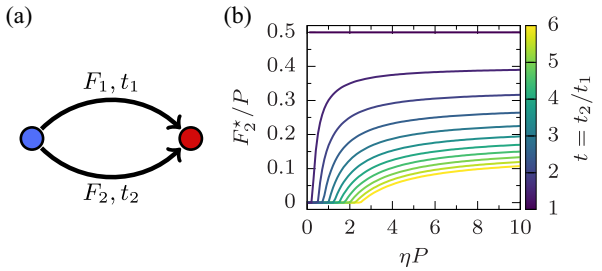

FIG. 8. Optimal flow in a network with congestion and two concurrent branches. Considering the case of a source (blue) and a sink (red) with an inflow and outflow of P, respectively.

APPENDIX: MORE GENERAL BENCHMARK

In this Appendix, we derive a general solution for the flows in a network with two concurrent branches as sketched in Fig. 8(a). We discuss the solution in dependence of the free-flow travel time ratio $t = t_2/t_1$ of the two branches and the congestion parameter η. In the following, we assume $t > 1$ w.l.o.g.

Denoting the inflow at the source with P, Kirchhoff's current law yields

$$F_1 + F_2 = P \Rightarrow F_1 = P - F_2.$$

Using $t := t_2/t_1$, the total travel time τ reads

$$\begin{aligned}\tau &= t_1\left(F_1 + \eta F_1^2\right) + t_2\left(F_2 + \eta F_2^2\right)\\ &= t_1\left[P - F_2 + \eta\left(P^2 - 2PF_2 + F_2^2\right) + t\left(F_2 + \eta F_2^2\right)\right]\\ &= t_1\left[\eta(1+t)F_2^2 - (1 + 2P\eta - t)F_2 + P + \eta P^2\right].\end{aligned}$$

For the optimal flow $F_2^\star$, the derivative of τ vanishes:

$$\partial_{F_2}\tau(F_2^\star) = t_1[2\eta(1+t)F_2^\star - (1 + 2P\eta - t)] \stackrel{!}{=} 0.$$

Hence,

$$F_2^\star = \frac{2P\eta + 1 - t}{2\eta(1+t)} = \frac{2\tilde{\eta} + 1 - t}{2\tilde{\eta}(1+t)}P,$$

with the rescaled congestion parameter $\tilde{\eta} := P\eta$. Considering the directedness constraint, $F_2 \geqslant 0$, we finally get

$$F_2^\star(\tilde{\eta}, t) = \begin{cases}\frac{2\tilde{\eta}+1-t}{2\tilde{\eta}(1+t)}P, & \tilde{\eta} > \frac{t-1}{2},\\ 0, & \text{else.}\end{cases} \tag{A1}$$

The optimal flow $F_2^\star$ thus depends both on the ratio t of the free-flow weight of both branches and the rescaled congestion

parameter $\tilde{\eta} = \eta P$. The critical congestion strength is

$$\tilde{\eta}_c = \eta_c P = \frac{t-1}{2}. \tag{A2}$$

Hence, the minimal congestion needed to activate a branch which has t times the weight of the shortest path increases linearly with t. In Fig. 8(b), $F_2^\star$ is plotted over $\tilde{\eta} = \eta P$ for different values of t. When passing the critical value of congestion $\tilde{\eta}_c$, the flow on the longer branch quickly increases at first and then slowly saturates towards $F_2^\star = P/(1+t)$ as $\tilde{\eta} \to \infty$.

[1] F. Corson, Fluctuations and Redundancy in Optimal Transport Networks, Phys. Rev. Lett. **104**, 048703 (2010).

[2] E. Katifori, G. J. Szöllősi, and M. O. Magnasco, Damage and Fluctuations Induce Loops in Optimal Transport Networks, Phys. Rev. Lett. **104**, 048704 (2010).

[3] D. P. Bebber, J. Hynes, P. R. Darrah, L. Boddy, and M. D. Fricker, Biological solutions to transport network design, Proc. R. Soc. London B **274**, 2307 (2007).

[4] A. Yazdani and P. Jeffrey, Complex network analysis of water distribution systems, Chaos **21**, 016111 (2011).

[5] G. Eiger, U. Shamir, and A. Ben-Tal, Optimal design of water distribution networks, Water Resour. Res. **30**, 2637 (1994).

[6] F. Kaiser, H. Ronellenfitsch, and D. Witthaut, Discontinuous transition to loop formation in optimal supply networks, Nat. Commun. **11**, 5796 (2020).

[7] M. T. Gastner and M. E. J. Newman, Optimal design of spatial distribution networks, Phys. Rev. E **74**, 016117 (2006).

[8] M. Barthélemy and A. Flammini, Optimal traffic networks, J. Stat. Mech.: Theory Exp. (2006) L07002.

[9] R. K. Ahuja, T. L. Magnanti, and J. B. Orlin, *Network Flows* (Prentice Hall, Upper Saddle River, NJ, 1993)

[10] G. Dantzig, R. Fulkerson, and S. Johnson, Solution of a large-scale traveling-salesman problem, J. Oper. Res. Soc. Am. **2**, 393 (1954).

[11] E. L. Lawler, J. K. Lenstra, A. H. G. R. Kan, and D. B.Shmoys, *The Traveling Salesman Problem: A Guided Tour of Combinatorial Optimization* (John Wiley & Sons, Hoboken, NJ, 1985).

[12] R. K. Ahuja, K. Mehlhorn, J. Orlin, and R. E. Tarjan, Faster algorithms for the shortest path problem, J. ACM **37**, 213 (1990).

[13] B. Bollobás, *Modern Graph Theory*, Graduate texts in mathematics, No. 184 (Springer, New York, NY, 1998).

[14] A. J. Wood, B. F. Wollenberg, and G. B. Sheblé, *Power Generation, Operation and Control* (John Wiley & Sons, New York, NY, 2014).

[15] A. E. Motter and Y.-C. Lai, Cascade-based attacks on complex networks, Phys. Rev. E **66**, 065102(R) (2002).

[16] P. Crucitti, V. Latora, and M. Marchiori, Model for cascading failures in complex networks, Phys. Rev. E **69**, 045104(R) (2004).

[17] J. Strake, F. Kaiser, F. Basiri, H. Ronellenfitsch, and D. Witthaut, Nonlocal impact of link failures in linear flow networks, New J. Phys. **21**, 053009 (2019).

[18] F. Kaiser, J. Strake, and D. Witthaut, Collective effects of link failures in linear flow networks, New J. Phys. **22**, 013053 (2020).

[19] S. Boyd and L. Vandenberghe, *Convex Optimization* (Cambridge University Press, New York, NY, 2004).

[20] K. Cheshmi, D. M. Kaufman, S. Kamil, and M. M. Dehnavi, NASOQ: Numerically accurate sparsity-oriented QP solver, ACM Trans. Graph. **39** (2020).

[21] K. Nagel and M. Schreckenberg, A cellular automaton model for freeway traffic, J. Phys. I (France) **2**, 2221 (1992).

[22] W. Klingsch, C. Rogsch, A. Schadschneider, and M. Schreckenberg, *Pedestrian and Evacuation Dynamics 2008* (Springer, Berlin, 2010).

[23] United States. Bureau of Public Roads, *Traffic assignment manual for application with a large, high speed computer*, Vol. 2 (U.S. Department of Commerce, Washington, D.C., 1964).

[24] R. Louf and M. Barthelemy, How congestion shapes cities: From mobility patterns to scaling, Sci. Rep. **4**, 5561 (2014).

[25] M. Newman, *Networks: An Introduction* (Oxford University Press, Oxford, UK, 2010).

[26] P. M. Pardalos and S. A. Vavasis, Quadratic programming with one negative eigenvalue is np-hard, J. Global Optim. **1**, 15 (1991).

[27] M. Kozlov, S. Tarasov, and L. Khachiyan, The polynomial solvability of convex quadratic programming, USSR Comput. Math. Math. Phys. **20**, 223 (1980).

[28] A. Nagurney and Q. Qiang, Robustness of transportation networks subject to degradable links, Europhys. Lett. **80**, 68001 (2007).

[29] Y. Sheffi, *Urban Transportation Networks*, Vol. 6 (Prentice-Hall, Englewood Cliffs, NJ, 1985).

[30] B. D. Greenshields, Studying traffic capacity by new methods, J. Appl. Psych. **20**, 353 (1936).

[31] H. Greenberg, An analysis of traffic flow, Oper. Res. **7**, 79 (1959).

[32] D. Helbing, Derivation and empirical validation of a refined traffic flow model, Physica A **233**, 253 (1996).

[33] D. Helbing, Fundamentals of traffic flow, Phys. Rev. E **55**, 3735 (1997).

[34] D. Helbing, Traffic and related self-driven many-particle systems, Rev. Mod. Phys. **73**, 1067 (2001).

[35] A. Schadschneider, Traffic flow: a statistical physics point of view, Physica A **313**, 153 (2002).

[36] R. Prud'homme, M. Koning, L. Lenormand, and A. Fehr, Public transport congestion costs: The case of the paris subway, Transport Policy **21**, 101 (2012).

[37] O. Cats, J. West, and J. Eliasson, A dynamic stochastic model for evaluating congestion and crowding effects in transit systems, Transport. Res. B: Methodol. **89**, 43 (2016).

[38] A. De Palma, M. Kilani, and S. Proost, Discomfort in mass transit and its implication for scheduling and pricing, Transport. Res. B: Methodol. **71**, 1 (2015).

[39] L. Haywood and M. Koning, The distribution of crowding costs in public transport: New evidence from paris, Transport. Res. A: Policy Pract. **77**, 182 (2015).

[40] L. Haywood, M. Koning, and R. Prud'Homme, The economic cost of subway congestion: Estimates from paris, Econ. Transport. **14**, 1 (2018).

[41] M. Yap, O. Cats, and B. van Arem, Crowding valuation in urban tram and bus transportation based on smart card data, Transport. A: Transport Sci. **16**, 23 (2020).

[42] M. de Lapparent and M. Koning, Analyzing time sensitivity to discomfort in the paris subway: An interval data model approach, Transportation **43**, 913 (2016).

[43] H. Stark and S. Schuster, Comparison of various approaches to calculating the optimal hematocrit in vertebrates, J. Appl. Physiol. **113**, 355 (2012).

[44] W. Kim and J. W. Bush, Natural drinking strategies, J. Fluid Mech. **705**, 7 (2012).

[45] K. H. Jensen, W. Kim, N. M. Holbrook, and J. W. Bush, Optimal concentrations in transport systems, J. R. Soc., Interface **10**, 20130138 (2013).

[46] T. H. Cormen, C. E. Leiserson, R. L. Rivest, and C. Stein, *Introduction to Algorithms* (MIT Press, Cambridge, MA, 2022).

[47] D. P. Bertsekas, *Constrained Optimization and Lagrange Multiplier Methods* (Academic Press, New York, NY, 1982).

[48] H. Cross, Analysis of flow in networks of conduits or conductors, Eng. Exper. Stat. Bull. **286** (1936).

[49] KVB, Bahnen-Schienennetz, https://www.kvb.koeln/fahrtinfo/liniennetzplaene.html#lightbox/0/ (2020).

[50] L. Haywood and M. Koning, Estimating crowding costs in public transport, DIW Berlin Discussion Paper, https://papers.ssrn.com/sol3/papers.cfm?abstract_id=2256332 (2013).

[51] A. Ermagun, S. Chatterjee, and D. Levinson, Using temporal detrending to observe the spatial correlation of traffic, PLoS One **12**, e0176853 (2017).

[52] F. Kaiser, V. Latora, and D. Witthaut, Network isolators inhibit failure spreading in complex networks, Nat. Commun. **12**, 3143 (2021).